UC Berkeley

Title

Omics-driven identification and elimination of valerolactam catabolism in Pseudomonas putida KT2440 for increased product titer

Permalink

Authors

Thompson, Mitchell G
Valencia, Luis E
Blake-Hedges, Jacquelyn M
et al.

Publication Date

DOI

Peer reviewed

Omics-driven identification and elimination of valerolactam catabolism in *Pseudomonas putida* KT2440 for increased product titer

Mitchell G. Thompson [a,b,c], Luis E. Valencia [a,b,d], Jacquelyn M. Blake-Hedges [a,b,e],
Pablo Cruz-Morales [a,b,f], Alexandria E. Velasquez [a,b], Allison N. Pearson [a,b],
Lauren N. Sermeno [a,b], William A. Sharpless [a,b], Veronica T. Benites [a,b], Yan Chen [a,b],
Edward E.K. Baidoo [a,b], Christopher J. Petzold [a,b], Adam M. Deutschbauer [c,g],
Jay D. Keasling [a,b,d,h,i,j,*]

[a] *Joint BioEnergy Institute, 5885 Hollis Street, Emeryville, CA, 94608, USA*
[b] *Biological Systems & Engineering Division, Lawrence Berkeley National Laboratory, Berkeley, CA, 94720, USA*
[c] *Department of Plant and Microbial Biology, University of California, Berkeley, CA, 94720, USA*
[d] *Joint Program in Bioengineering, University of California, Berkeley/San Francisco, CA, 94720, USA*
[e] *Department of Chemistry, University of California, Berkeley, CA, 94720, USA*
[f] *Centro de Biotecnologia FEMSA, Instituto Tecnologico y de Estudios Superiores de Monterrey, Mexico*
[g] *Environmental Genomics and Systems Biology Division, Lawrence Berkeley National Laboratory, Berkeley, CA, USA*
[h] *Department of Chemical and Biomolecular Engineering, University of California, Berkeley, CA, 94720, USA*
[i] *The Novo Nordisk Foundation Center for Biosustainability, Technical University of Denmark, Denmark*
[j] *Center for Synthetic Biochemistry, Institute for Synthetic Biology, Shenzhen Institutes for Advanced Technologies, Shenzhen, China*

A B S T R A C T

Pseudomonas putida is a promising bacterial chassis for metabolic engineering given its ability to metabolize a wide array of carbon sources, especially aromatic compounds derived from lignin. However, this omnivorous metabolism can also be a hindrance when it can naturally metabolize products produced from engineered pathways. Herein we show that *P. putida* is able to use valerolactam as a sole carbon source, as well as degrade caprolactam. Lactams represent important nylon precursors, and are produced in quantities exceeding one million tons per year (Zhang et al., 2017). To better understand this metabolism we use a combination of Random Barcode Transposon Sequencing (RB-TnSeq) and shotgun proteomics to identify the *oplBA* locus as the likely responsible amide hydrolase that initiates valerolactam catabolism. Deletion of the *oplBA* genes prevented *P. putida* from growing on valerolactam, prevented the degradation of valerolactam in rich media, and dramatically reduced caprolactam degradation under the same conditions. Deletion of *oplBA*, as well as pathways that compete for precursors L-lysine or 5-aminovalerate, increased the titer of valerolactam from undetectable after 48 h of production to ~90 mg/L. This work may serve as a template to rapidly eliminate undesirable metabolism in non-model hosts in future metabolic engineering efforts.

1. Introduction

Pseudomonas putida has attracted great attention as a potential chassis organism for metabolic engineering due in large part to its ability to metabolize a wide variety of carbon sources, particularly aromatic compounds that can be derived from lignin (Loeschcke and Thies, 2015; Ravi et al., 2017). To more fully realize this vision, much effort has been put forth recently to better characterize the central metabolism of *P. putida* with updated genome-scale models (Nogales et al., 2017), C[13] flux experiments (Kukurugya et al., 2019; Nikel et al., 2015), and high-throughput fitness assays, which have all contributed to a more complete understanding of the bacterium (Thompson et al., 2019a; Rand et al., 2017). Despite these advances, the metabolic capabilities of *P. putida* are not yet fully understood.

One consequence of this omnivorous metabolism is that *P. putida* possesses the ability to degrade or fully catabolize chemicals metabolic engineers seek to produce in the host. An ongoing challenge for *P. putida* host engineering is to rapidly identify catabolic pathways of important target molecules and eliminate them from the genome. The recent report of a novel pathway for levulinic acid catabolism in *P. putida* KT2440 underscores the catabolic flexibility of the host, and an additional obstacle towards producing high product titer (Rand et al., 2017). While challenging, this is not surprising; as a genus, *Pseudomonads* are well known for their ability to degrade a wide range of naturally occurring or

xenobiotic chemicals (Clarke, 1982; George and Hay, 2011).

Caprolactam and valerolactam are both important commodity chemicals used in the synthesis of nylon polymers, with global production of caprolactam reaching over four million metric tons (Zhang et al., 2017). Multiple efforts have been made to produce these chemicals biologically, with the titers of valerolactam approaching 1 g/L in *Escherichia coli* (Zhang et al., 2017; Chae et al., 2017). The engineered pathway to valerolactam in *E. coli* converts L-lysine to 5-aminovalerate (5AVA) via DavBA, two genes endogenous to *P. putida*, and then cyclizes it via a promiscuous coA-ligase (Zhang et al., 2017). While the endogenous L-lysine catabolism of *P. putida* has been leveraged to produce the C5 diacid glutarate, there has yet to be any attempt to produce valerolactam in the bacterium (Zhang et al., 2018). It has previously been put forth that *P. putida* can catabolize valerolactam and caprolactam (Belda et al., 2016). Furthermore, a recent report that *Pseudomonas jessenii* can catabolize caprolactam suggested that catabolism of lactams could dramatically impact titers of valerolactam in *P. putida* (Otzen et al., 2018).

In this work we demonstrate that *P. putida* can utilize valerolactam as a sole carbon source, as well as degrade caprolactam. Using a combination of Random Barcode Transposon Sequencing (RB-TnSeq) and shotgun proteomics we were able to identify that OplBA, a predicted oxoprolinase, is responsible for this hydrolysis. By knocking out *oplBA* in addition to two pathways that compete for precursors we were able to increase the titers of valerolactam in *P. putida*.

2. Results

2.1. Identification of a lactam hydrolase in P. putida

The hydrolysis product of valerolactam is 5AVA, an intermediate in L-lysine metabolism (Fig. 1A). Growth curves of *P. putida* on valerolactam as a sole carbon source demonstrated that the bacterium was readily able to catabolize valerolactam and produce biomass, with growth similar to that on either 5AVA and glucose (Fig. 1B). *P. putida* was also able to use both valerolactam and caprolactam as a sole nitrogen source (Fig. S1). Initially, we attempted to identify the enzyme responsible for valerolactam hydrolysis using RB-TnSeq, a technique that has previously been used to identify novel enzymes in D-lysine metabolism (Thompson et al., 2019a). RB-TnSeq measures the relative fitness of transposon mutant pools to infer gene function through changes in relative abundance of all non-essential genes in a bacterium under a selective condition (Wetmore et al., 2015; Price et al., 2018). Mutant pools of *P. putida* were grown on either 5AVA or valerolactam as a sole carbon source in an attempt to identify enzymes solely essential for growth on valerolactam. Results of RB-TnSeq experiments suggested that valerolactam was indeed being catabolized through the same pathway as 5AVA with both conditions showing significant defects in the *davTD* and *csiD-lghO* operons, the
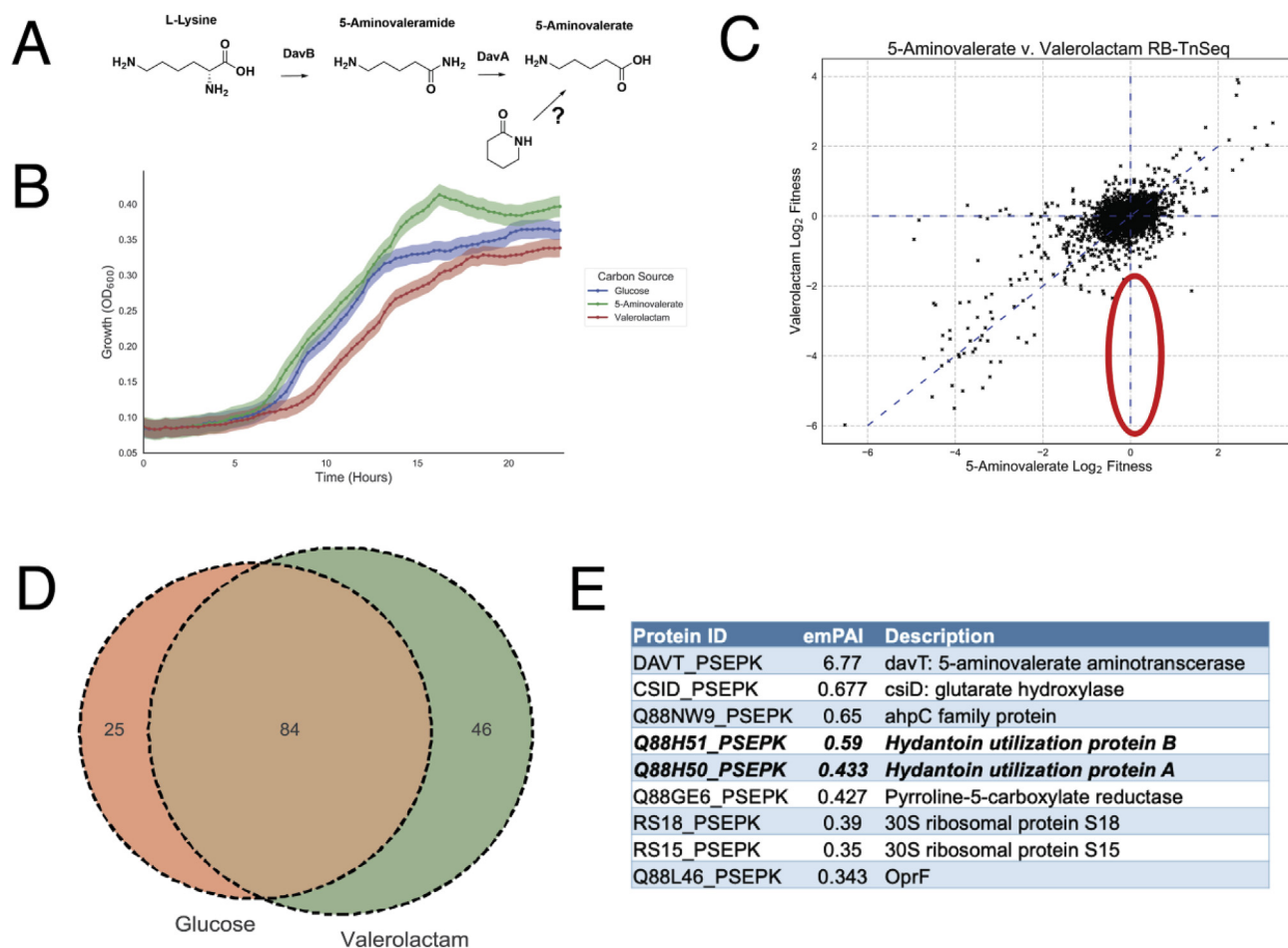

Figure 1. Identification of the *P. putida* valerolactam hydrolase: (A) Route of valerolactam catabolism through the L-lysine catabolic route of *P. putida* (B) Growth of *P. putida* in minimal medium supplemented with either 10 mM glucose, 5AVA, or valerolactam. Shaded area represents the 95% confidence interval (cI), n = 3. Maximal growth rates (1/hr) were 0.29 on glucose, 0.29 on 5AVA, and 0.21 on valerolactam. (C) RB-TnSeq analysis of genome fitness assays of *P. putida* libraries grown on either 5AVA or valerolactam as a sole carbon source. Red oval shows the predicted fitness result of a valerolactam hydrolase. (D) Results of shotgun proteomics of proteins found in the supernatant of *P. putida* grown on either 10 mM glucose or 10 mM valerolactam as a sole carbon source. Venn diagram shows the number of proteins with an exponentially modified protein abundance index (emPAI) relative abundance above 0.1 shared or unique to each carbon source (E) Table shows the most abundant proteins specific to grown on valerolactam. OplA (Q88H50_PSEPK) and OplB (Q88H51_PSEPK) are in bold.

known catabolic route of 5AVA to the TCA cycle (Fig. S2A). However, there were no genes that showed obvious fitness defects only under the valerolactam growth condition (Fig. 1C).

The inability of the RB-TnSeq approach to identify the hydrolytic enzyme could result from the enzyme being secreted from the cell. In this case, the secreted enzymes from cells containing the intact hydrolase gene produce 5AVA which can freely diffuse into hydrolase mutant cells, eliminating any selective pressure for lactam-based growth. To test whether the enzymes responsible for lactam hydrolysis may be secreted, cultures of *P. putida* were either grown on glucose or valerolactam as a sole carbon source, their supernatants filtered, concentrated, and then subjected to shotgun proteomics. Of the most abundant proteins in the supernatant, there were 25 proteins that were specific to glucose, while 46 were specific to valerolactam, with 86 proteins being shared between the two conditions (Fig. 1D). Within the top five most abundant proteins in the valerolactam supernatant were OplB (Q88H51_PSEPK) and OplA (Q88H51_PSEPK), which together are annotated as the two subunits of a 5-oxoprolinase, orthologs of which have been suggested to participate in the caprolactam catabolism of *P. jessenii* (Fig. 1E) (Otzen et al., 2018). Additional shotgun proteomics of cell pellets grown on either glucose, 5AVA, or valerolactam showed that OplB and OplA were more highly expressed in the presence of the lactam in comparison to the other carbon sources (Fig. S2C). Interestingly, fitness data from two valerolactam RB-TnSeq experiments in *P. putida* KT2440 show *oplBA* mutants having no significant fitness defects (Fig. S2B). Orthologs of *oplBA* are widely distributed across many bacteria including other attractive metabolic engineering chassis such as *Rhodococcus opacus*, and are nearly always located adjacent to one another on the genome (Fig. S3).

2.2. Deletion of oplBA mitigates consumption of valerolactam and caprolactam

To confirm the role of OplBA in the catabolism of valerolactam, deletions were constructed of the *oplBA* locus in *P. putida* via homologous recombination. Growth of the mutant was compared to the wild type as well as to a deletion mutant of *davT*, which catalyzes the first step in 5AVA catabolism. All strains showed identical growth on glucose as a sole carbon source (Fig. 2A). In the presence of 5AVA the *oplBA* deletion strain showed no growth defect compared to the wild-type, while the *davT* mutant predictably was unable to grow (Fig. 2B). However, on valerolactam only the wild type strain grew, while both the *oplBA* and *davT* mutants showed no measurable growth after 40 h (Fig. 2C). Growth rates of strains on all carbon sources are reported in Table S1. Complementation of *oplBA* mutants with *oplBA* expressed from a plasmid restored growth on valerolactam, while a sham plasmid expressing RFP was unable to grow (Fig. S4). These results suggest that OplBA is the sole enzyme responsible for the conversion of valerolactam to 5AVA under these conditions.

While *P. putida* KT2440 can utilize valerolactam as a sole carbon source, it is unable to grow on caprolactam (data not shown). In order to determine whether the OplBA of *P. putida* is capable of degrading other lactams, wild type and Δ*oplBA* strains were grown in LB medium supplemented with 10 mM caprolactam, valerolactam, or butyrolactam for 24 h after which the remaining lactam concentration was compared to an uninoculated medium control. Wild type *P. putida* consumed all detectable valerolactam within 24 h, and less than 50% of both butyrolactam and caprolactam remained compared to the uninoculated control (Fig. 2D). There was no significant decrease in amount of valerolactam in the Δ*oplBA* cultures compared to the uninoculated control (*t*-test of $p = 0.178$), though there was a slight but significant decrease of 0.74 mM caprolactam (*t*-test of $p = 0.033$). No butyrolactam remained in the Δ*oplBA* culture after 24 h (Fig. 2D). This result was surprising as the annotated substrate of OplBA, 5-oxoproline, has the same ring size as butyrolactam. Previous work has shown that homologs of OplBA are ATP-dependent amidohydrolases that hydrolyze 5-oxoproline (Seddon et al., 1985). However, when purified OplBA was incubated with valerolactam in addition to ATP and magnesium we observed no hydrolysis relative to boiled enzyme controls (Fig. S5).
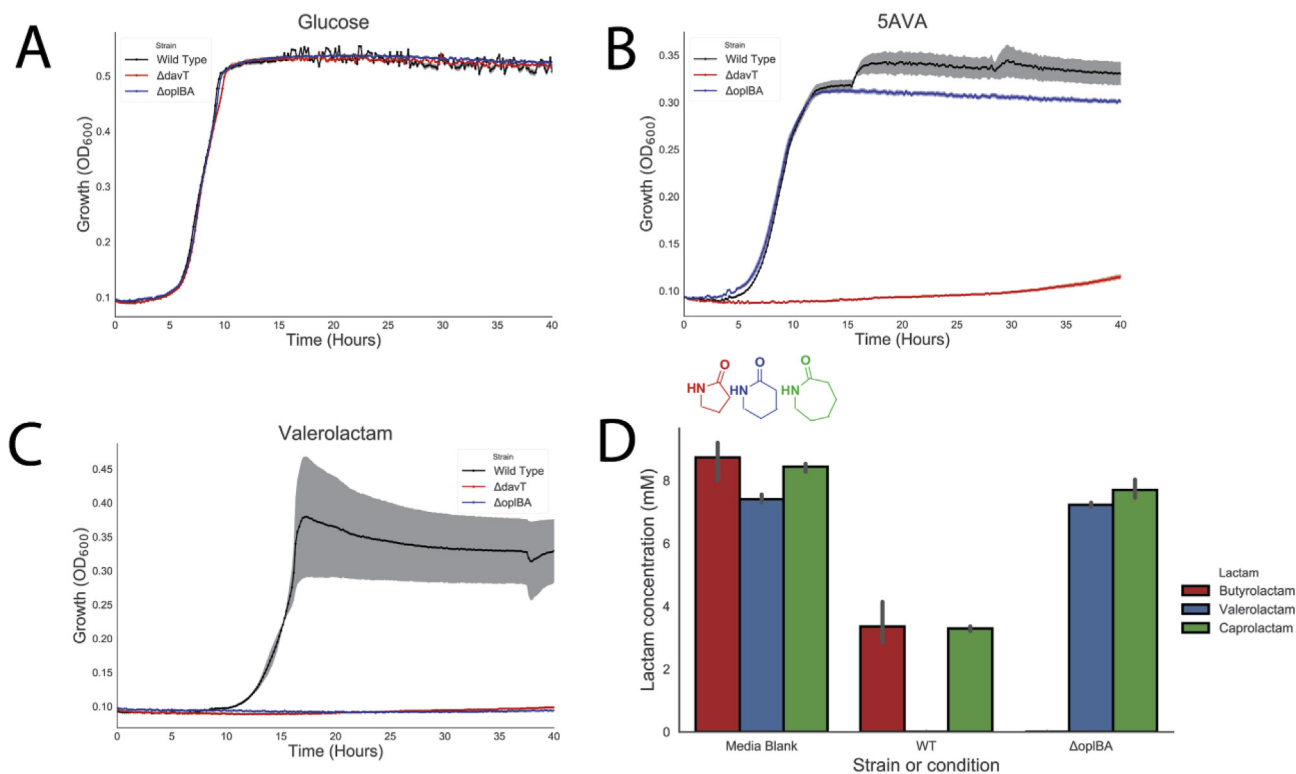

Figure 2. OplBA controls valerolactam and caprolactam degradation in *P. putida*. Growth of wild-type, Δ*davT*, or Δ*oplBA* in minimal media supplemented with either 10 mM glucose (A), 5-aminovaleroate (B), or valerolactam (C). (D) Remaining butyrolactam, valerolactam, or caprolactam in LB medium after 24-h incubation with no *P. putida*, wild-type, or a Δ*oplBA* mutant.

2.3. Host engineering for increased valerolactam production

The published pathway for the production of valerolactam from L-lysine in *E. coli* utilized the formation of 5AVA via the *davBA* pathway native to *P. putida*, followed by cyclization to the lactam via a promiscuous acyl-coA ligase from *Streptomyces aizunensis* (Fig. 3A) (Zhang et al., 2017). To produce valerolactam in *P. putida*, not only will the production pathway need to be overexpressed, but the *oplBA* locus and pathways that compete for 5AVA must be eliminated. Loss of flux to valerolactam occurs through two known competing pathways: the Alr-mediated isomerization to D-lysine or catabolism of 5AVA to glutarate via the action of DavTD (Fig. 3A) (Thompson et al., 2019a).

To investigate the relative contributions of pathways that contribute to either lactam hydrolysis or loss of substrate, we expressed the *davBA-ORF26* pathway via a arabinose-inducible broad host range vector pBADT in backgrounds where these pathways had been sequentially deleted. Wild type *P. putida* produced 0.43 mg/L valerolactam after 24 h, but no valerolactam could be detected after 48 h, presumably due to host consumption (Fig. 3B). Simple deletion of the *oplBA* locus resulted in a

10-fold increase of production at 24 h to 4.47 mg/L and a 48-h titer of 9.27 mg/L (Fig. 3B). Additional deletion of *davT* resulted in an increase of titer to 19.29 mg/L and 85.19 mg/L, and by deleting the amino acid racemase *alr* titers increased to 63.66 mg/L and 91.97 mg/L at 24 and 48 h, respectively (Fig. 3B).

3. Discussion

Recent economic analyses highlight the necessity of lignin valorization to create a sustainable bioeconomy (Baral et al., 2019; Becker and Wittmann, 2019). With its robust aromatic metabolism combined with novel methods of biomass deconstruction, *P. putida* has great potential to convert lignocellulosic biomass to value-added products (Rodriguez et al., 2017; Kohlstedt et al., 2018). Though the ability of *P. putida* to catabolize many carbon sources is often viewed as an asset, it has well documented metabolic pathways to degrade many compounds that metabolic engineers may wish to produce such as levulinic acid (Rand et al., 2017), various alcohols (Wehrmann et al., 2017), and the diacid glutarate (Zhang et al., 2018). As these catabolic phenotypes are
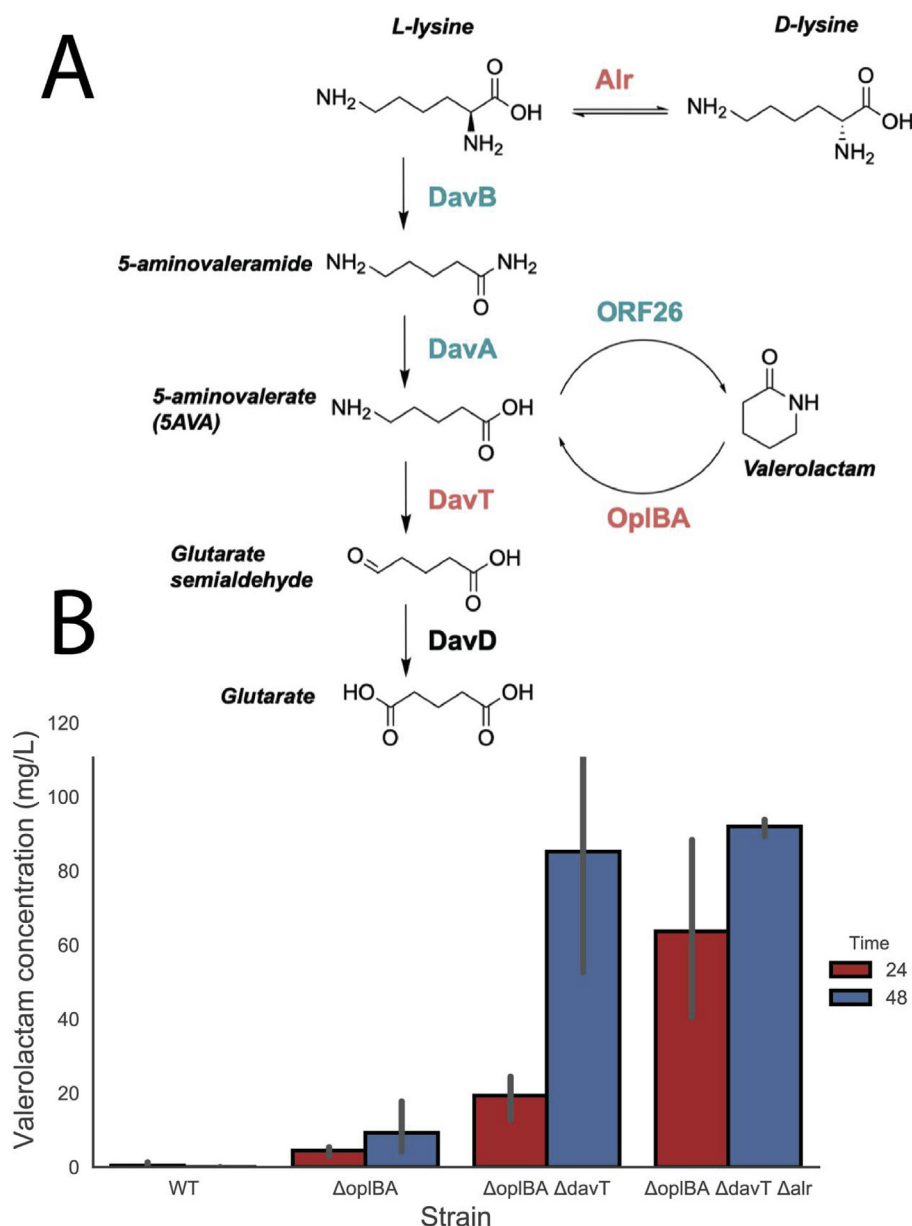
Figure 3. Production of valerolactam in *P. putida*: (A) Design of valerolactam producing *P. putida*. The biosynthetic pathway genes are shown in green and were overexpressed heterologously from a pBBR ori plasmid using an arabinose inducible promoter. Pathways that catabolize products or divert precursors are shown in red. (B) Valerolactam production from different *P. putida* strains grown in LB medium supplemented with 25 mM L-lysine and 0.2% (w/v) arabinose at 24 and 48 h post inoculation. Error bars show 95% cI, n = 3.

encountered it will be critical to rapidly identify the offending genomic loci.

The recent surge in development of functional genomics techniques has dramatically increased the throughput at which we can identify the genetic basis of unknown metabolism. RB-TnSeq has been used to uncover novel glutarate and levulinic acid metabolism, though was ineffective at identifying the *oplBA* locus (Thompson et al., 2019a; Rand et al., 2017). Proteomics techniques have also grown more robust, and were used in *P. jessenii* to predict a route of caprolactam catabolism (Otzen et al., 2018; Chen et al., 2019). Here, proteomics also proved to be an effective means of identifying the enzyme responsible for the hydrolysis of the lactam. Our proteomics results showed that OplBA was specifically expressed when grown on valerolactam, but not 5AVA. These results suggest that *P. putida* may have lactam-specific transcription factors which could be developed into valuable tools for metabolic engineering if identified.

The inability of RB-TnSeq to identify these genes is curious as single deletion mutants were unable to grow on valerolactam. A possible explanation for this is that OplBA may be secreted, which would create a public pool of 5AVA which *oplBA* mutants could still utilize. However, OplBA orthologs have been shown to be ATP-dependent (Seddon et al., 1985), which would be inconsistent with this extracellular localization. Unfortunately our attempts to characterize OplBA *in vitro* were unsuccessful, preventing us from identifying the substrate requirements of the enzyme. Though we were unable to reconstitute the activity of OplBA *in vitro*, deletion of *oplBA* did not prevent the degradation of butyrolactam which is a 5-membered lactam ring. The annotated function of the *oplBA* loci is a 5-oxoprolinase, which hydrolyzes the 5-membered lactam ring of 5-oxoproline. These results may suggest that the OplBA may function naturally as something other than a 5-oxoprolinase. More work will be necessary to resolve the results of our RB-TnSeq and feeding experiments to elucidate the biochemical requirements of OplBA as well as to better understand its cellular localization.

To achieve titers of ~90 mg/L we supplemented media with 25 mM L-lysine (3.65 g/L). Previous work in *E. coli* achieved titers of ~200 mg/L by feeding 1 g/L lysine and ~300 mg/L by feeding 5 g/L after 48 h (Zhang et al., 2017). Our results indicate that with significant host engineering, *P. putida* can produce titers approaching those of model organisms. Optimization of pathway expression could narrow this gap even further and should be a focus of future efforts.

While this initial work is encouraging, it still requires the feeding of L-lysine in rich media for conversion to valerolactam. Ideally, engineering *P. putida* would be able to metabolize lignin hydrolysis products directly to L-lysine on the way to the final product. A great deal of work has been conducted to elucidate the complex catabolism of lysine in *P. putida* (Thompson et al., 2019a; Zhang et al., 2018), yet relatively little work has been done to increase flux to lysine within the bacterium. While there has been little to divert flux to L-lysine in *P. putida*, there is a wealth of evidence in other bacteria where high titers of intracellular lysine have been achieved (Nærdal et al., 2011; Rajvanshi et al., 2013). The ever increasing body of research to characterize the sprawling metabolism of *P. putida* will greatly aid in future efforts of efficient production of valerolactam from lignocellulosic feedstocks.

4. Methods

4.1. Media, chemicals, and culture conditions

General *E. coli* cultures were grown in lysogeny broth (LB) Miller medium (BD Biosciences, USA) at 37 °C while P. putida was grown at 30 °C. When indicated, P. putida and E. coli were grown on modified MOPS minimal medium, which is comprised of 32.5 μM CaCl₂, 0.29 mM K₂SO₄, 1.32 mM K₂HPO₄, 8 μM FeCl₂, 40 mM MOPS, 4 mM tricine, 0.01 mM FeSO₄, 9.52 mM NH₄Cl, 0.52 mM MgCl₂, 50 mM NaCl, 0.03 μM (NH₄)₆Mo₇O₂₄, 4 μM H₃BO₃, 0.3 μM CoCl₂, 0.1 μM CuSO₄, 0.8 μM MnCl₂, and 0.1 μM ZnSO₄ (LaBauve and Wargo, 2012). Cultures were

supplemented with kanamycin (50 mg/L, Sigma Aldrich, USA), gentamicin (30 mg/L, Fisher Scientific, USA), or carbenicillin (100 mg/L, Sigma Aldrich, USA), when indicated. All other compounds were purchased through Sigma Aldrich (Sigma Aldrich, USA).

4.2. Strains and plasmids

All bacterial strains and plasmids used in this work are listed in Table 1. All strains and plasmids created in this work are available through the public instance of the JBEI registry. (public-registry.jbei.org/folders/456). All plasmids were designed using Device Editor and Vector Editor software, while all primers used for the construction of plasmids were designed using j5 software (Ham et al., 2012; Chen et al., 2012; Hillson et al., 2012). Plasmids were assembled via Gibson Assembly using standard protocols (Gibson et al., 2009), or Golden Gate Assembly using standard protocols (Engler et al., 2008). Plasmids were routinely isolated using the Qiaprep Spin Miniprep kit (Qiagen, USA), and all primers were purchased from Integrated DNA Technologies (IDT, Coralville, IA). Construction of *P. putida* deletion mutants was performed as described previously (Thompson et al., 2019a).

4.3. Plate based growth assays

Growth studies of bacterial strains were conducted a microplate reader kinetic assays. Overnight cultures were inoculated into 10 mL of LB medium from single colonies, and grown at 30 °C. These cultures were then washed twice with MOPS minimal media without any added carbon and diluted 1:100 into 500 μL of MOPS medium with 10 mM of a carbon source in 48-well plates (Falcon, 353072). Plates were sealed with a gas-permeable microplate adhesive film (VWR, USA), and then optical density and fluorescence were monitored for 48 h in an Biotek Synergy 4 plate reader (BioTek, USA) at 30 °C with fast continuous shaking. Optical density was measured at 600 nm.

4.4. Production assays and lactam quantification

To assess valerolactam production in strains of *P. putida* overnight cultures of strains harboring pBADT-*davBA-ORF26* were grown in 3 mL of LB supplemented with kanamycin and grown at 30 °C. Production cultures of 10 mL of LB supplemented with kanamycin, 25 mM L-lysine, and 0.2% w/v arabinose were then inoculated 1:100 with overnight cultures and then grown at 30 °C shaking at 250 rpm. Samples for valerolactam production were taken at 24 and 48 h post-inoculation, with 200 μL of culture being quenched with an equal volume of ice cold methanol and then stored at −20 °C until analysis.

For measurement of lactams, liquid chromatographic separation was

Table 1
Strains and plasmids used in this study.

Strain	JBEI Part ID	Reference
E. coli DH10B		Grant et al. (1990)
E. coli BL21(DE3)		Novagen
P. putida KT2440		ATCC 47054
P. putida ΔdavT		Thompson et al. (2019b)
P. putida ΔoplBA	JPUB_013576	This work
P. putida ΔoplBAΔdavT	JPUB_013577	This work
P. putida ΔoplBAΔdavTΔalr	JPUB_013578	This work
Plasmids		
pET28		Novagen
pET28 *oplA*	JPUB_013579	This work
pET28 *oplB*	JPUB_013581	This work
pBADT		Bi et al. (2013)
pBADT-*davBA*-ORF26	JPUB_013587	This work
pBADT-*oplBA*	JPUB_013620	This work
pMQ30		Shanks et al. (2009)
pMQ30 *oplBA*	JPUB_013585	This work
pMQ30 *alr*	JPUB_013583	This work
pMQ30 davT		Thompson et al. (2019b)

conducted at 20 °C with a Kinetex HILIC column (50-mm length, 4.6-mm internal diameter, 2.6-μm particle size; Phenomenex, Torrance, CA) using a 1260 Series HPLC system (Agilent Technologies, Santa Clara, CA, USA). The injection volume for each measurement was 5 μL. The mobile phase was composed of 10 mM ammonium formate and 0.07% formic acid in water (solvent A) and 10 mM ammonium formate and 0.07% formic acid in 90% acetonitrile and 10% water (solvent B) (HPLC grade, Honeywell Burdick & Jackson, CA, USA). High purity ammonium formate and formic acid (98–100% chemical purity) were purchased from Sigma-Aldrich, St. Louis, MO, USA. Lactams were separated with the following gradient: decreased from 90%B to 70%B in 2 min, held at 70%B for 0.75 min, decreased from 70%B to 40%B in 0.25 min, held at 40%B for 1.25 min, increased from 40%B to 90%B for 0.25 min, held at 90%B for 1 min. The flow rate was varied as follows: 0.6 mL/min for 3.25 min, increased from 0.6 mL/min to 1 mL/min in 0.25 min, and held at 1 mL/min for 2 min. The total run time was 5.5 min.

The HPLC system was coupled to an Agilent Technologies 6520 quadrupole time-of-flight mass spectrometer (QTOF MS) with a 1:6 post-column split. Nitrogen gas was used as both the nebulizing and drying gas to facilitate the production of gas-phase ions. The drying and nebulizing gases were set to 12 L/min and 30 lb/in^2, respectively, and a drying gas temperature of 350 °C was used throughout. Fragmentor, skimmer and OCT 1 RF voltages were set to 100 V, 50 V and 300 V, respectively. Electrospray ionization (ESI) was conducted in the positive-ion mode for the detection of $[M + H]^+$ ions with a capillary voltage of 4000 V. The collision energy voltage was set to 0 V. MS experiments were carried out in the full-scan mode (75–1100 m/z) at 0.86 spectra/s. The QTOF-MS system was tuned with the Agilent ESI-L Low concentration tuning mix in the range of 50–1700 m/z. Lactams were quantified by comparison with 8-point calibration curves of authentic chemical standards from 0.78125 μM to 100 μM. R^2 coefficients of ≥ 0.99[EB1] were achieved for the calibration curves. Data acquisition was performed by Agilent MassHunter Workstation (version B.05.00), qualitative assessment by Agilent MassHunter Qualitative Analysis (version B.05.00 or B.06.00), and data curation by Agilent Profinder (version B.08.00).

4.5. RB-TnSeq and proteomics analysis

RB-TnSeq experiments utilized *P. putida* library JBEI-1 which has been described previously (Thompson et al., 2019a). Libraries of JBEI-1 were thawed on ice, diluted into 25 mL of LB medium with kanamycin and then grown to an OD$_{600}$ of 0.5 at 30 °C at which point three 1 mL aliquots were removed, pelleted, and stored at −80 °C. Libraries were then washed once in MOPS minimal medium with no carbon source, and then diluted 1:50 in MOPS minimal medium with 10 mM valerolactam. Cells were grown in 500 μL of medium in 48-well plates (Falcon, 353072). Plates were sealed with a gas-permeable microplate adhesive film (VWR, USA), and then grown at 30 °C in a Tecan Infinite F200 microplate reader (Tecan Life Sciences, San Jose, CA), with shaking at 200 rpm. Two 500 μL aliquots were combined, pelleted, and stored at −80 °C until BarSeq analysis, which was performed as previously described (Rand et al., 2017; Wetmore et al., 2015). All fitness data is publically available at http://fit.genomics.lbl.gov.

Secreted proteins of *P. putida* were prepared by growing 500 mL of culture in MOPS minimal medium supplemented with either 10 mM glucose or 10 mM valerolactam for 24 h at 30 °C, which were subsequently pelleted and filtered through a 0.22 μm filter and then concentrated 100x via a 10 kD MW cutoff filter. Cultures for intracellular proteomics analysis were grown in 10 mL cultures in the same conditions on either glucose, 5AVA, or valerolactam and were then pelleted and stored at −80 °C until sample workup and proteomic analysis. Proteins from secreted and intracellular samples were desalted and isolated using a variation of a previously-described chloroform/methanol extraction protocol (Wessel and Flügge, 1984). For secreted proteins, 100–200 μL of the concentrated protein sample was used; for intracellular samples, cell pellets were thoroughly resuspended in 100 μL HPLC water. Then, the

following reagents were added to each sample in sequential order with thorough vortexing after each addition: 400 μL of HPLC grade methanol, 100 μL of HPLC grade chloroform, 300 μL of HPLC grade water. Samples were centrifuged for 1 min at ~21,000 g in order to promote phase separation. After centrifugation, the entirety of the top layer (water and methanol) was removed and discarded, leaving on the protein pellet and chloroform layer remaining. Another 300 μL of HPLC grade methanol was added, then the samples were vortexed and centrifuged again for 2 min at ~21,000 g. The remaining liquid was then removed and discarded, and the cell pellets were allowed to dry in a fume hood for 5 min. Protein pellets were then resuspended in freshly-prepared 100 mM ammonium bicarbonate buffer in HPLC water containing 20% HPLC methanol. Protein concentrations in the resuspended samples were quantified using a DC Protein Assay Kit (Bio-Rad Laboratories, Hercules, CA). After quantification, 100 μg of protein was transferred to a PCR strip and tris(2-carboxyethyl)phosphine was added to a final concentration of 5 mM. Samples were incubated at 22 °C for 30 min, after which iodoacetamide was added (final concentration 10 mM). Samples were again incubated at 22 °C in the dark for 30 min. Finally, trypsin was added to a final ratio of 1:25 w/w trypsin:sample, and samples were digested at 37 °C for 5–8 h before being transferred to conical LC vials for LC-MS analysis. Peptides prepared for shotgun proteomic experiments were analyzed by using an Agilent 6550 iFunnel Q-TOF mass spectrometer (Agilent Technologies, Santa Clara, CA) coupled to an Agilent 1290 UHPLC system as described previously (González Fernández-Niño et al., 2015). 20 μg of peptides were separated on a Sigma–Aldrich Ascentis Peptides ES-C18 column (2.1 mm × 100 mm, 2.7 μm particle size, operated at 60 °C) at a 0.400 mL/min flow rate and eluted with the following gradient: initial condition was 98% solvent A (0.1% formic acid v/v) and 2% solvent B (99.9% acetonitrile, 0.1% formic acid v/v). Solvent B was increased to 35% over 30 min, and then increased to 80% over 2 min, then held for 6 min, followed by a ramp back down to 2% B over 1 min where it was held for 4 min to re-equilibrate the column to original conditions. Peptides were introduced to the mass spectrometer from the LC by using a Jet Stream source (Agilent Technologies) operating in positive-ion mode (3500 V). Source parameters employed gas temp (250 °C), drying gas (14 L/min), nebulizer (35 psig), sheath gas temp (250 °C), sheath gas flow (11 L/min), VCap (3500 V), fragmentor (180 V), OCT 1 RF Vpp (750 V). The data were acquired with Agilent MassHunter Workstation Software, LC/MS Data Acquisition B.06.01 operating in Auto MS/MS mode whereby the 20 most intense ions (charge states, 2–5) within 300–1400 m/z mass range above a threshold of 1500 counts were selected for MS/MS analysis. MS/MS spectra (100–1700 m/z) were collected with the quadrupole set to "Medium" resolution and were acquired until 45,000 total counts were collected or for a maximum accumulation time of 333 ms. Former parent ions were excluded for 0.1 min following MS/MS acquisition. The acquired data were exported as mgf files and searched against the latest *P. putida* KT2440 protein database with Mascot search engine version 2.3.02 (Matrix Science). The resulting search results were filtered and analyzed by Scaffold v 4.3.0 (Proteome Software Inc.).

4.6. Protein purification and biochemical analysis of OplBA

Both *oplB* and *oplA* were cloned into the expression vector pET28 harboring N-terminal 6x-histidine purification tags. Protein expression and purification were carried out as described previously (Thompson et al., 2019a). To characterize activity of OplBA we used conditions that were previously described to characterize 5-oxoprolinase with minor changes (Li et al., 1988). Briefly, 10 μM of each OplB and OplA or boiled controls were incubated for 4 h at 30 °C with 2 mM valerolactam in 100 mM Tris-HCl pH 7.0, 4 mM MgCl$_2$, with or without 2 mM ATP. Reactions were quenched with ice-cold methanol, filtered through a 3 kDa MWCO filter, diluted 40-fold with 50% methanol/50% H2O v/v, and stored at - 20 °C until analysis via LC-MS.

4.7. Bioinformatic analyses

All statistical analyses were carried out using either the Python Scipy or Numpy libraries (Jones, Oliphant, Peterson; van der Walt et al., 2011). For the phylogenetic reconstructions, the best amino acid substitution model was selected using ModelFinder as implemented on IQ-tree (Kalyaanamoorthy et al., 2017) phylogenetic trees were constructed using IQ-tree, nodes were supported with 10,000 bootstrap replicates. The final tree figures were edited using FigTree v1.4.3 (http://tree.bio.ed.ac.uk/software/figtree/). Orthologous syntenic regions of OplBA were identified with CORASON-BGC (Cruz-Morales et al., 2017) and manually colored and annotated.

Acknowledgements

Appendix A. Supplementary data

Supplementary data to this article can be found online at https://doi.org/10.1016/j.mec.2019.e00098.

Contributions

Conceptualization, M.G.T.; Methodology, M.G.T., L.E.V.,J.M.B, P.C.M.,E.E.K.B.; Investigation, M.G.T., L.E.V., J.M.B, P.C.M, V.T.B, W.A.S., A.N.P., A.E.V.; Writing – Original Draft, M.G.T.; Writing – Review and Editing, All authors.; Resources and supervision, C.J.P., A.M.D., J.D.K.

Conflicts of interest

J.D.K. has financial interests in Amyris, Lygos, Demetrix, Napigen and Maple Bio.

References

Baral, N., Kavvada, O., Perez, D.M., Mukhopadhyay, A., Lee, T.S., Simmons, B., et al., 2019. Techno-economic analysis and life-cycle greenhouse gas mitigation cost of five routes to bio-jet fuel blendstocks. Energy Environ. Sci. https://doi.org/10.1039/C8EE03266A.

Becker, J., Wittmann, C., 2019. A field of dreams: lignin valorization into chemicals, materials, fuels, and health-care products. Biotechnol. Adv. https://doi.org/10.1016/j.biotechadv.2019.02.016.

Belda, E., van Heck, R.G.A., José Lopez-Sanchez, M., Cruveiller, S., Barbe, V., Fraser, C., et al., 2016. The revisited genome of Pseudomonas putida KT2440 enlightens its value as a robust metabolic chassis. Environ. Microbiol. 18, 3403–3424. https://doi.org/10.1111/1462-2920.13230.

Bi, C., Su, P., Müller, J., Yeh, Y.-C., Chhabra, S.R., Beller, H.R., et al., 2013. Development of a broad-host synthetic biology toolbox for Ralstonia eutropha and its application to engineering hydrocarbon biofuel production. Microb. Cell Factories 12, 107. https://doi.org/10.1186/1475-2859-12-107.

Chae, T.U., Ko, Y.-S., Hwang, K.-S., Lee, S.Y., 2017. Metabolic engineering of Escherichia coli for the production of four-, five- and six-carbon lactams. Metab. Eng. 41, 82–91. https://doi.org/10.1016/j.ymben.2017.04.001.

Chen, J., Densmore, D., Ham, T.S., Keasling, J.D., Hillson, N.J., 2012. Device Editor visual biological CAD canvas. J. Biol. Eng. 6, 1. https://doi.org/10.1186/1754-1611-6-1.

Chen, Y., Vu, J., Thompson, M.G., Sharpless, W.A., Chan, L.J.G., Gin, J.W., et al., 2019. A rapid methods development workflow for high-throughput quantitative proteomic applications. PLoS One 14, e0211582. https://doi.org/10.1371/journal.pone.0211582.

Clarke, P.H., 1982. The metabolic versatility of pseudomonads. Antonie Leeuwenhoek 48, 105–130. https://doi.org/10.1007/BF00405197.

Cruz-Morales, P., Ramos-Aboites, H.E., Licona-Cassani, C., Selem-Mójica, N., Mejía-Ponce, P.M., Souza-Saldívar, V., et al., 2017. Actinobacteria phylogenomics, selective isolation from an iron oligotrophic environment and siderophore functional characterization, unveil new desferrioxamine traits. FEMS Microbiol. Ecol. 93 https://doi.org/10.1093/femsec/fix086.

Engler, C., Kandzia, R., Marillonnet, S., 2008. A one pot, one step, precision cloning method with high throughput capability. PLoS One 3, e3647. https://doi.org/10.1371/journal.pone.0003647.

George, K.W., Hay, A.G., 2011. Bacterial strategies for growth on aromatic compounds. Adv. Appl. Microbiol. 74, 1–33. https://doi.org/10.1016/B978-0-12-387022-3.00005-7.

Gibson, D.G., Young, L., Chuang, R.-Y., Venter, J.C., Hutchison, C.A., Smith, H.O., 2009. Enzymatic assembly of DNA molecules up to several hundred kilobases. Nat. Methods 6, 343–345. https://doi.org/10.1038/nmeth.1318.

González Fernández-Niño, S.M., Smith-Moritz, A.M., Chan, L.J.G., Adams, P.D., Heazlewood, J.L., Petzold, C.J., 2015. Standard flow liquid chromatography for shotgun proteomics in bioenergy research. Front. Bioeng. Biotechnol. 3, 44. https://doi.org/10.3389/fbioe.2015.00044.

Grant, S.G., Jessee, J., Bloom, F.R., Hanahan, D., 1990. Differential plasmid rescue from transgenic mouse DNAs into Escherichia coli methylation-restriction mutants. Proc. Natl. Acad. Sci. U.S.A. 87, 4645–4649.

Ham, T.S., Dmytriv, Z., Plahar, H., Chen, J., Hillson, N.J., Keasling, J.D., 2012. Design, implementation and practice of JBEI-ICE: an open source biological part registry platform and tools. Nucleic Acids Res. 40, e141. https://doi.org/10.1093/nar/gks531.

Hillson, N.J., Rosengarten, R.D., Keasling, J.D., 2012. j5 DNA assembly design automation software. ACS Synth. Biol. 1, 14–21. https://doi.org/10.1021/sb2000116.

E. Jones, T. Oliphant, P. Peterson, Others, SciPy: Open Source Scientific Tools for Python, (n.d).

Kalyaanamoorthy, S., Minh, B.Q., Wong, T.K.F., von Haeseler, A., Jermiin, L.S., 2017. ModelFinder: fast model selection for accurate phylogenetic estimates. Nat. Methods 14, 587–589. https://doi.org/10.1038/nmeth.4285.

Kohlstedt, M., Starck, S., Barton, N., Stolzenberger, J., Selzer, M., Mehlmann, K., et al., 2018. From lignin to nylon: cascaded chemical and biochemical conversion using metabolically engineered Pseudomonas putida. Metab. Eng. 47, 279–293. https://doi.org/10.1016/j.ymben.2018.03.003.

Kukurugya, M.A., Mendonca, C.M., Solhtalab, M., Wilkes, R.A., Thannhauser, T.W., Aristilde, L., 2019. Multi-omics analysis unravels a segregated metabolic flux network that tunes co-utilization of sugar and aromatic carbons in Pseudomonas putida. J. Biol. Chem. https://doi.org/10.1074/jbc.RA119.007885.

LaBauve, A.E., Wargo, M.J., 2012. Growth and laboratory maintenance of Pseudomonas aeruginosa (Chapter 6). Curr. Protoc. Microbiol Unit 6E.1. https://doi.org/10.1002/9780471729259.mc06e01s25.

Li, L.Y., Seddon, A.P., Meister, A., 1988. Interaction of the protein components of 5-oxoprolinase. Substrate-dependent enzyme complex formation. J. Biol. Chem. 263, 6495–6501.

Loeschcke, A., Thies, S., 2015. Pseudomonas putida-a versatile host for the production of natural products. Appl. Microbiol. Biotechnol. 99, 6197–6214. https://doi.org/10.1007/s00253-015-6745-4.

Nikel, P.I., Chavarría, M., Fuhrer, T., Sauer, U., de Lorenzo, V., 2015. Pseudomonas putida KT2440 strain metabolizes glucose through a cycle formed by enzymes of the entner-doudoroff, embden-meyerhof-parnas, and pentose phosphate pathways. J. Biol. Chem. 290, 25920–25932. https://doi.org/10.1074/jbc.M115.687749.

Nogales, J., Gudmundsson, S., Duque, E., Ramos, J.L., Palsson, B.O., 2017. Expanding the Computable Reactome in Pseudomonas Putida Reveals Metabolic Cycles Providing Robustness. BioRxiv. https://doi.org/10.1101/139121.

Nærdal, I., Netzer, R., Ellingsen, T.E., Brautaset, T., 2011. Analysis and manipulation of aspartate pathway genes for L-lysine overproduction from methanol by Bacillus methanolicus. Appl. Environ. Microbiol. 77, 6020–6026. https://doi.org/10.1128/AEM.05093-11.

Otzen, M., Palacio, C., Janssen, D.B., 2018. Characterization of the caprolactam degradation pathway in Pseudomonas jessenii using mass spectrometry-based

proteomics. Appl. Microbiol. Biotechnol. 102, 6699–6711. https://doi.org/10.1007/s00253-018-9073-7.

Price, M.N., Wetmore, K.M., Waters, R.J., Callaghan, M., Ray, J., Liu, H., et al., 2018. Mutant phenotypes for thousands of bacterial genes of unknown function. Nature 557, 503–509. https://doi.org/10.1038/s41586-018-0124-0.

Rajvanshi, M., Gayen, K., Venkatesh, K.V., 2013. Lysine overproducing Corynebacterium glutamicum is characterized by a robust linear combination of two optimal phenotypic states. Syst. Synth. Biol. 7, 51–62. https://doi.org/10.1007/s11693-013-9107-5.

Rand, J.M., Pisithkul, T., Clark, R.L., Thiede, J.M., Mehrer, C.R., Agnew, D.E., et al., 2017. A metabolic pathway for catabolizing levulinic acid in bacteria. Nat. Microbiol. 2, 1624–1634. https://doi.org/10.1038/s41564-017-0028-z.

Ravi, K., García-Hidalgo, J., Gorwa-Grauslund, M.F., Lidén, G., 2017. Conversion of lignin model compounds by Pseudomonas putida KT2440 and isolates from compost. Appl. Microbiol. Biotechnol. 101, 5059–5070. https://doi.org/10.1007/s00253-017-8211-y.

Rodriguez, A., Salvachúa, D., Katahira, R., Black, B.A., Cleveland, N.S., Reed, M., et al., 2017. Base-catalyzed depolymerization of solid lignin-rich streams enables microbial conversion. ACS Sustain. Chem. Eng. 5, 8171–8180. https://doi.org/10.1021/acssuschemeng.7b01818.

Seddon, A.P., Li, L., Meister, A., 1985. [54] 5-Oxo-l-prolinase from Pseudomonas putida. In: Glutamate, Glutamine, Glutathione, and Related Compounds. Elsevier, pp. 451–458. https://doi.org/10.1016/S0076-6879(85)13057-0.

Shanks, R.M.Q., Kadouri, D.E., MacEachran, D.P., O'Toole, G.A., 2009. New yeast recombineering tools for bacteria. Plasmid 62, 88–97. https://doi.org/10.1016/j.plasmid.2009.05.002.

Thompson, M.G., Blake-Hedges, J.M., Cruz-Morales, P., Barajas, J.F., Curran, S.C., Eiben, C.B., et al., 2019. Massively parallel fitness profiling reveals multiple novel enzymes in Pseudomonas putida lysine metabolism. mBio 10. https://doi.org/10.1128/mBio.02577-18.

Thompson, M.G., Cruz-Morales, P., Krishna, R.N., Blake-Hedges, J.M., Incha, M.R., Keasling, J.D., 2019. Glutarate metabolism in Pseudomonas putida is regulated by two distinct glutarate sensing transcription factors. BioRxiv. https://doi.org/10.1101/557751.

van der Walt, S., Colbert, S.C., Varoquaux, G., 2011. The NumPy array: a structure for efficient numerical computation. Comput. Sci. Eng. 13, 22–30. https://doi.org/10.1109/MCSE.2011.37.

Wehrmann, M., Billard, P., Martin-Meriadec, A., Zegeye, A., Klebensberger, J., 2017. Functional role of lanthanides in enzymatic activity and transcriptional regulation of pyrroloquinoline quinone-dependent alcohol dehydrogenases in Pseudomonas putida KT2440. mBio 8. https://doi.org/10.1128/mBio.00570-17.

Wessel, D., Flügge, U.I., 1984. A method for the quantitative recovery of protein in dilute solution in the presence of detergents and lipids. Anal. Biochem. 138, 141–143. https://doi.org/10.1016/0003-2697(84)90782-6.

Wetmore, K.M., Price, M.N., Waters, R.J., Lamson, J.S., He, J., Hoover, C.A., et al., 2015. Rapid quantification of mutant fitness in diverse bacteria by sequencing randomly bar-coded transposons. mBio 6, e00306–e00315. https://doi.org/10.1128/mBio.00306-15.

Zhang, J., Barajas, J.F., Burdu, M., Wang, G., Baidoo, E.E., Keasling, J.D., 2017. Application of an acyl-CoA ligase from Streptomyces aizunensis for lactam biosynthesis. ACS Synth. Biol. 6, 884–890. https://doi.org/10.1021/acssynbio.6b00372.

Zhang, M., Gao, C., Guo, X., Guo, S., Kang, Z., Xiao, D., et al., 2018. Increased glutarate production by blocking the glutaryl-CoA dehydrogenation pathway and a catabolic pathway involving L-2-hydroxyglutarate. Nat. Commun. 9, 2114. https://doi.org/10.1038/s41467-018-04513-0.